

# Detection of deuterated methylcyanoacetylene, CH<sub>2</sub>DC<sub>3</sub>N, in TMC-1

★

C. Cabezas<sup>1</sup>, E. Roueff<sup>2</sup>, B. Tercero<sup>3,4</sup>, M. Agúndez<sup>1</sup>, N. Marcelino<sup>1</sup>, P. de Vicente<sup>3</sup> and J. Cernicharo<sup>1</sup>

<sup>1</sup> Grupo de Astrofísica Molecular, Instituto de Física Fundamental (IFF-CSIC), C/ Serrano 121, 28006 Madrid, Spain. e-mail: carlos.cabezas@csic.es; jose.cernicharo@csic.es

<sup>2</sup> LERMA, Observatoire de Paris, PSL Research University, CNRS, Sorbonne Universités, 92190 Meudon, France

<sup>3</sup> Observatorio Astronómico Nacional (IGN), C/ Alfonso XII, 3, 28014, Madrid, Spain.

<sup>4</sup> Centro de Desarrollos Tecnológicos, Observatorio de Yebes (IGN), 19141 Yebes, Guadalajara, Spain.

Received; accepted

## ABSTRACT

We report the first detection in space of the single deuterated isotopologue of methylcyanoacetylene, CH<sub>2</sub>DC<sub>3</sub>N. A total of fifteen rotational transitions, with  $J = 8-12$  and  $K_a = 0$  and 1, were identified for this species in TMC-1 in the 31.0-50.4 GHz range using the Yebes 40m radio telescope. The observed frequencies were used to derive for the first time the spectroscopic parameters of this deuterated isotopologue. We derive a column density of  $(8.0 \pm 0.4) \times 10^{10} \text{ cm}^{-2}$ . The abundance ratio between CH<sub>3</sub>C<sub>3</sub>N and CH<sub>2</sub>DC<sub>3</sub>N is  $\sim 22$ . We also theoretically computed the principal spectroscopic constants of <sup>13</sup>C isotopologues of CH<sub>3</sub>C<sub>3</sub>N and CH<sub>3</sub>C<sub>4</sub>H and those of the deuterated isotopologues of CH<sub>3</sub>C<sub>4</sub>H for which we could expect a similar degree of deuteration enhancement. However, we have not detected either CH<sub>2</sub>DC<sub>4</sub>H nor CH<sub>3</sub>C<sub>4</sub>D nor any <sup>13</sup>C isotopologue. The different observed deuterium ratios in TMC-1 are reasonably accounted for by a gas phase chemical model where the low temperature conditions favor deuterium transfer through reactions with H<sub>2</sub>D<sup>+</sup>.

**Key words.** Astrochemistry — ISM: molecules — ISM: individual (TMC-1) — line: identification — molecular data

## 1. Introduction

Deuterium fractionation is a well-known process in the dense interstellar medium which can occur both in the gas phase and on the surfaces of dust particles. This process allows deuterated isotopic species of interstellar molecules to reach abundances much higher than the D/H elemental abundance ratio ( $1.5 \times 10^{-5}$  Linsky 2003). The high efficiency of deuterium fractionation allows deuterated species to achieve abundances as high as 30-40 % relative to the parent species, as occurs with HDCS (Marcelino et al. 2005) and CH<sub>2</sub>DOH (Parise et al. 2006). Hence, deuterated isotopologues of abundant interstellar molecules make a significant contribution to the spectral richness of line surveys. This fact makes the astronomical identification of these isotopologues of utmost importance, not only to gain knowledge on their molecular formation pathways or how deuterium fractionation works, but also to assign unidentified features in line surveys.

Very sensitive broadband line surveys of astronomical sources can now be achieved thanks to new technical developments on radiotelescopes. These surveys have boosted up the number of new molecular identifications in the last years, because weak lines arising from low-abundance species and from low-dipole moment species can be now easily detected (Agúndez et al. 2021a; Cernicharo et al. 2021a,b,c). The negative counterpart of this high sensitivity is the huge number of new lines which populate the survey, including isotopologues and vibrationally excited states, in warm environments, of well known

species. Hence, discovering spectral features of new molecules requires a previous detailed analysis of the spectral contribution of known species.

Methylcyanoacetylene, CH<sub>3</sub>C<sub>3</sub>N, also known as cyanopropyne or methylpropionitrile, has been detected with high abundance in the cold dark cloud TMC-1 (Brotten 1984) and more recently by Marcelino et al. (2021) using a high sensitivity line survey on TMC-1 gathered with the Yebes 40m radio telescope (see, e.g., Cernicharo et al. 2021d). Hence, the deuterated isotopologues of CH<sub>3</sub>C<sub>3</sub>N are good candidates to be observed in this source using the same line survey. In fact, we have already detected other singly deuterated isotopologues of species such as CH<sub>3</sub>CN, CH<sub>3</sub>CCH, *c*-C<sub>3</sub>H<sub>2</sub>, C<sub>4</sub>H, H<sub>2</sub>C<sub>4</sub>, H<sub>2</sub>CCN, HC<sub>3</sub>N and HC<sub>5</sub>N (Cabezas et al. 2021).

In this Letter we report the identification of spectral lines of the deuterated species CH<sub>2</sub>DC<sub>3</sub>N in TMC-1. Our search for this molecule is based on the change in the rotational parameters of CH<sub>3</sub>C<sub>3</sub>N produced by the H/D exchange, which have been obtained by ab initio calculations. The derived deuterium ratios are confronted to an extended chemical model including the related deuterated compounds.

## 2. Observations

The Q-band observations of TMC-1 ( $\alpha_{J2000} = 4^{\text{h}}41^{\text{m}}41.9^{\text{s}}$  and  $\delta_{J2000} = +25^{\circ}41'27.0''$ ) described in this work were performed in several sessions between November 2019 and April 2021. They were carried out using a set of new receivers, built within

\* Based on observations carried out with the Yebes 40m telescope (projects 19A003, 20A014, and 20D15). The 40m radiotelescope at Yebes Observatory is operated by the Spanish Geographic Institute (IGN, Ministerio de Transportes, Movilidad y Agenda Urbana).

the Nanocosmos project<sup>1</sup>, and installed at the Yebes 40m radio telescope.

The Q-band receiver consists of two high electron mobility transistor cold amplifiers covering the 31.0-50.4 GHz band in horizontal and vertical polarizations. The receiver temperature varies from 22 K at 32 GHz to 42 K at 50 GHz. The spectrometers formed by  $2 \times 8 \times 2.5$  GHz FFTs provide a spectral resolution of 38.15 kHz and cover the whole Q-band in both polarizations. The receivers and the spectrometers are described before by Ter-cero et al. (2021).

Different frequency coverages were observed, 31.08-49.52 GHz and 31.98-50.42 GHz, which permits to check that no spurious ghosts are produced in the down-conversion chain in which the signal coming from the receiver is downconverted to 1-19.5 GHz, and then splits into 8 bands with a coverage of 2.5 GHz, each of which being analyzed by the FFTs.

The observing procedure used was the frequency switching mode, with a frequency throw of 10 MHz or 8 MHz (see, e.g., Cernicharo et al. 2021d,e,f).

The intensity scale, antenna temperature ( $T_A^*$ ), was calibrated using two absorbers at different temperatures and the atmospheric transmission model ATM (Cernicharo 1985; Pardo et al. 2001). Calibration uncertainties have been adopted to be 10 % based on the observed repeatability of the line intensities between different observing runs. All data have been analyzed using the GILDAS package<sup>2</sup>.

### 3. Results

The identification of most of the features from our TMC-1 Q-band line survey was done using the MADEX code (Cernicharo 2012) and the CDMS and JPL catalogues (Müller et al. 2005; Pickett et al. 1998). Nevertheless many lines remain unidentified. Among these U-lines we found a series of five lines with a harmonic relation 8:9:10:11:12 between them. This series of lines could be fitted using a Hamiltonian for a linear molecule obtaining accurate values for  $B$  and  $D$  constants;  $B = 1989.428172 \pm 0.000610$  MHz and  $D = 0.10950 \pm 0.00269$  kHz. However, a deeper inspection of the survey around the mentioned lines revealed the presence of two additional series of lines at higher and lower frequencies from the first series. The spectral pattern, taking into account all the lines, is easily recognizable as the typical  $a$ -type transition spectrum of a near-prolate molecule, with the sets of rotational transitions containing  $J+1_{0,J+1} \leftarrow J_{0,J}$ ,  $J+1_{1,J+1} \leftarrow J_{1,J}$  and  $J+1_{1,J} \leftarrow J_{1,J-1}$  separated by  $B+C$ . All the observed lines, shown in Table 1 and Fig. 1, were analyzed using an asymmetric rotor Hamiltonian in the FITWAT code (Cernicharo et al. 2018) to derive the rotational and centrifugal distortion constants shown in Table 2. With the available data we could not determine the  $A$  rotational constant, which was kept fixed to the ab initio value, as explained below.

The identification of the spectral carrier is first based on the following points. (i) The molecule is a closed-shell species without any appreciable fine or hyperfine interaction or large amplitude motion. (ii) The determined values for  $B$  and  $C$  constants indicate that the molecule is a very slightly asymmetric rotor, because  $B$  and  $C$  values are similar. (iii) The  $(B+C)/2$  value (1989.43 MHz, corresponding to the rotational constant of the close symmetric species) is smaller than that of  $H_2C_5$  (2295.29 MHz) but larger than that of  $H_2C_6$  (1344.72 MHz), which indicates that the molecule should contain four C atoms

**Table 1.** Observed line parameters for  $CH_2DC_3N$  in TMC-1.

$(J_{K_a,K_c})_u - (J_{K_a,K_c})_l$	$\nu_{obs}^a$ (MHz)	$\int T_A^* dv^b$ (mK km s <sup>-1</sup> )	$\Delta\nu^c$ (km s <sup>-1</sup> )	$T_A^*$ (mK)
8 <sub>1,8</sub> – 7 <sub>1,7</sub>	31797.891	2.08±0.12	0.84±0.15	2.3±0.4
8 <sub>0,8</sub> – 7 <sub>0,7</sub>	31830.626	2.76±0.07	0.79±0.11	3.3±0.4
8 <sub>1,7</sub> – 7 <sub>1,6</sub>	31862.950	1.39±0.20	0.70±0.12	1.9±0.4
9 <sub>1,9</sub> – 8 <sub>1,8</sub>	35772.575	1.67±0.14	0.64±0.11	2.5±0.4
9 <sub>0,9</sub> – 8 <sub>0,8</sub>	35809.389	3.11±0.04	0.69±0.06	4.3±0.3
9 <sub>1,8</sub> – 8 <sub>1,7</sub>	35845.744	1.31±0.16	0.74±0.14	3.1±0.3
10 <sub>1,10</sub> – 9 <sub>1,9</sub>	39747.236	0.73±0.30	0.45±0.15	1.6±0.4
10 <sub>0,10</sub> – 9 <sub>0,9</sub>	39788.132	2.66±0.06	0.67±0.07	3.8±0.4
10 <sub>1,9</sub> – 9 <sub>1,8</sub>	39828.533	1.07±0.34	0.62±0.16	1.6±0.4
11 <sub>1,11</sub> – 10 <sub>1,10</sub>	43721.867	1.45±0.33	0.73±0.32	1.9±0.4
11 <sub>0,11</sub> – 10 <sub>0,10</sub>	43766.845	2.11±0.10	0.47±0.09	4.2±0.4
11 <sub>1,10</sub> – 10 <sub>1,9</sub>	43811.297	1.77±0.24	0.98±0.35	1.7±0.4
12 <sub>1,12</sub> – 11 <sub>1,11</sub>	47696.518	0.86±0.40	0.82±0.20	2.1±0.5
12 <sub>0,12</sub> – 11 <sub>0,11</sub>	47745.519	1.91±0.10	0.46±0.06	3.9±0.5
12 <sub>1,11</sub> – 11 <sub>1,10</sub>	47794.026	0.83±0.46	0.45±0.11	1.7±0.5

**Notes.** <sup>(a)</sup> Observed frequencies towards TMC-1 for which we adopted a  $v_{LSR}$  of 5.83 km s<sup>-1</sup> (Cernicharo et al. 2020a,b,c). The frequency uncertainty 10 kHz. <sup>(b)</sup> Integrated line intensity in mK km s<sup>-1</sup>. <sup>(c)</sup> Line width at half intensity derived by fitting a Gaussian function to the observed line profile (in km s<sup>-1</sup>).

**Table 2.** Observationally derived and theoretical spectroscopic parameters (in MHz) for  $CH_2DC_3N$ .

Constant	Space <sup>a</sup>	Ab initio <sup>b</sup>
$A$	120120.70 <sup>c</sup>	120120.70
$B$	1993.493107(593)	1993.53
$C$	1985.363112(657)	1985.74
$\Delta_J$	9.107(230) 10 <sup>-5</sup>	-
$\Delta_{JK}$	1.4767(249) 10 <sup>-2</sup>	-
$rms^d$	13.6	-
$J_{min}/J_{max}$	8/12	-
$K_{min}/K_{max}$	0/1	-
$N^e$	15	-

**Notes.** <sup>(a)</sup> Fit to the lines of  $CH_2DC_3N$  observed in TMC-1. <sup>(b)</sup> CCSD/cc-pVTZ level of theory. Scaled values using as reference  $CH_3C_3N$ . See text. <sup>(c)</sup> Fixed to the calculated value. <sup>(d)</sup> The standard deviation of the fit in kHz. <sup>(e)</sup> Number of lines included in the fit.

and one atom heavier than C. With these assumptions, we excluded species with four C atoms and a sulfur atom because they are too heavy. Species containing four C atoms and oxygen, like  $HC_4O$  (Kohguchi et al. 1994) and  $H_2C_4O$  (Brown et al. 1979) are rejected as candidates because they are too light ( $B=2279.914$  MHz and  $(B+C)/2=2153.75$  MHz, respectively) and other species derived from them are too heavy or open-shell species. Molecules with four C atoms and nitrogen could be good candidates.  $HC_4N$  (Tang et al. 1999) has a rotational constant  $B=2302.398$  MHz and  $(B+C)/2$  values for the cationic species  $HC_4NH^+$  and  $H_2C_4N^+$  in their  $^1\Sigma$  electronic ground states have been calculated to be 2159.3 MHz and 2194.7 MHz, respectively (CCSD/cc-pVTZ level of theory; Cížek 1969; Dunning 1989). The next member of this hydrogen addition progression is  $CH_3C_3N$ , whose rotational constant is 2065.74 MHz, very close to our  $(B+C)/2$  value. This fact prompted us to think that the spectral carrier could be the deuterated isotopologue  $CH_2DC_3N$ , an asymmetric rotor, because the H/D interchange breaks the  $C_{3v}$  symmetry of  $CH_3C_3N$ .

We performed geometry optimization calculations for  $CH_3C_3N$  and  $CH_2DC_3N$ , in order to estimate the isotopic shift on the rotational constants for the  $CH_3C_3N/CH_2DC_3N$  system. Using experimental/theoretical ratios is the most common method to predict the expected experimental rotational constants

<sup>1</sup> <https://nanocosmos.iff.csic.es/>

<sup>2</sup> <http://www.iram.fr/IRAMFR/GILDAS>

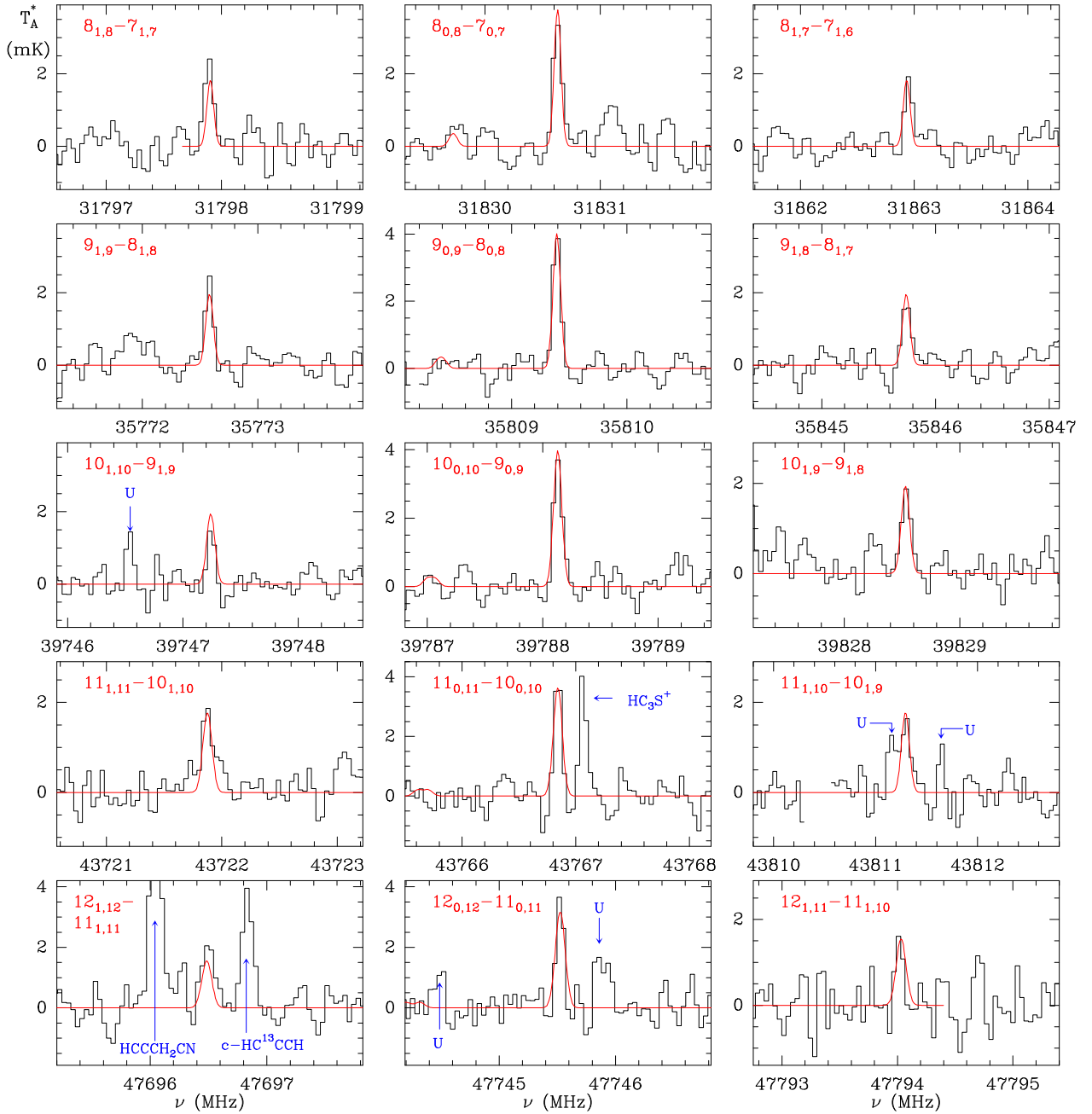


**Fig. 1.** Observed lines of CH<sub>2</sub>DC<sub>3</sub>N in TMC-1 in the 31.0-50.4 GHz range. Frequencies and line parameters are given in Table 1. Quantum numbers for the observed transitions are indicated in each panel. The red line shows the synthetic spectrum computed for a rotational temperature of 8 K and a column density of  $8 \times 10^{10} \text{ cm}^{-2}$  (see text). The additional components seen in the synthetic spectrum close to the  $K_a = 0$  components are the  $K_a = 2$  rotational transitions. Blanked channels correspond to negative features created in the folding of the frequency switching data. The label U corresponds to features above  $4\sigma$ .

for an isotopic species of a given molecule when the rotational constants for its parent species are known. Hence, we employed the CCSD/cc-pVTZ level of theory (Cížek 1969; Dunning 1989) which reproduces well the  $B$  rotational constant for CH<sub>3</sub>C<sub>3</sub>N, 2058.0 MHz *vs.* 2065.74 MHz. The theoretical values for the rotational constants of CH<sub>2</sub>DC<sub>3</sub>N were then scaled using the experimental/theoretical ratio obtained from CH<sub>3</sub>C<sub>3</sub>N, and the results are shown in Table 2. As it can be seen, the predicted values for CH<sub>2</sub>DC<sub>3</sub>N perfectly match with those derived from our fit, which allows us to conclude that the spectral carrier of our lines is CH<sub>2</sub>DC<sub>3</sub>N. It should be noted that the calculations provide the equilibrium values for the rotational constants ( $A_e$ ,

$B_e$  and  $C_e$ ), while the experimental values are the ground state rotational constants ( $A_0$ ,  $B_0$  and  $C_0$ ). In spite that the equilibrium rotational constants slightly differ from the ground state constants, we can assume similar discrepancies for CH<sub>3</sub>C<sub>3</sub>N and CH<sub>2</sub>DC<sub>3</sub>N and, thus, the estimated constants for CH<sub>2</sub>DC<sub>3</sub>N are essentially unaffected by this fact.

Methyldiacetylene (CH<sub>3</sub>C<sub>4</sub>H) is 7.5 times more abundant than, and lines have similar intensities to, CH<sub>3</sub>C<sub>3</sub>N (Marcelino et al. 2021; Cernicharo et al. 2021c). Hence, it is straightforward to think that spectral signatures of the deuterated species of CH<sub>3</sub>C<sub>4</sub>H could also be detected in our line survey. We followed the same strategy used for CH<sub>2</sub>DC<sub>3</sub>N to predict the transition

**Table 3.** Predicted spectroscopic constants<sup>a</sup> (in MHz) for isotopic species of CH<sub>3</sub>C<sub>3</sub>N and CH<sub>3</sub>C<sub>4</sub>H.

Species	<i>B</i>
<sup>13</sup> CH <sub>3</sub> CCCN	2010.51
CH <sub>3</sub> <sup>13</sup> CCCN	2054.75
CH <sub>3</sub> C <sup>13</sup> CCN	2065.71
CH <sub>3</sub> CC <sup>13</sup> CN	2048.72
CH <sub>3</sub> CCC <sup>15</sup> N	2011.56
<sup>13</sup> CH <sub>3</sub> CCCCH	1982.60
CH <sub>3</sub> <sup>13</sup> CCCCH	2025.34
CH <sub>3</sub> C <sup>13</sup> CCCH	2035.71 <sup>c</sup>
CH <sub>3</sub> CC <sup>13</sup> CCH	2018.90
CH <sub>3</sub> CCC <sup>13</sup> CH	1980.28
CH <sub>2</sub> DCCCCH <sup>b</sup>	<i>A</i> = 120899.40 <i>B</i> = 1965.96 <i>C</i> = 1958.41

**Notes.** <sup>(a)</sup> For all the <sup>13</sup>C and <sup>15</sup>N species it can be assumed the *A* value for the corresponding parent species, CH<sub>3</sub>C<sub>3</sub>N or CH<sub>3</sub>C<sub>4</sub>H, 158099.0 and 159140.0 MHz, respectively. <sup>(b)</sup> *A*, *B* and *C* constants are provided due to the C<sub>s</sub> symmetry of this species. <sup>(c)</sup> For this isotopologue laboratory data are available (Cazzoli et al. 2008). The experimental rotational constant *B* is 2035.67752 MHz.

frequencies of CH<sub>2</sub>DC<sub>4</sub>H. Laboratory values are available for CH<sub>3</sub>C<sub>4</sub>D (Heath et al. 1955). We carried out geometry optimization calculations for CH<sub>3</sub>C<sub>4</sub>H. The rotational constants obtained for CH<sub>2</sub>DC<sub>4</sub>H are shown in Table 3. We found only two lines at the predicted transition frequencies corresponding to the 8<sub>0,8</sub>-7<sub>0,7</sub> and 9<sub>0,9</sub>-8<sub>0,8</sub> with intensities ~ 1 mK. Other lines predicted in the frequency range of the line survey are below the present sensitivity. We consider that the deuterated isotopologue of CH<sub>3</sub>C<sub>4</sub>H is not detected so far (see below). The deuteration of this species is discussed in the following section.

Considering the intensity of the CH<sub>3</sub>C<sub>3</sub>N and CH<sub>3</sub>C<sub>4</sub>H lines in our line survey, we also expected to observe the <sup>13</sup>C isotopologues as well. The frequency transitions for these species were predicted using the rotational constants from Table 3, which were obtained using the same procedure employed for the CH<sub>2</sub>DC<sub>3</sub>N isotopic species. However, we could not find spectral signatures for any of these species around the predicted frequencies.

The column density of CH<sub>2</sub>DC<sub>3</sub>N has been derived from a rotational diagram analysis of the observed intensities. We have assumed a source of uniform brightness with a radius of 40'' (Fossé et al. 2001). We derive  $T_r = 8 \pm 0.5$  K and  $N(\text{CH}_2\text{DC}_3\text{N}) = (8.0 \pm 0.4) \times 10^{10} \text{ cm}^{-2}$ . As shown in Fig. 1 the agreement between the synthetic spectrum and the observations is excellent. The column density is not very sensitive to the adopted value of the rotational temperature between 6 and 10 K. For the normal isotopologue Marcelino et al. (2021) derived a rotational temperature for the *A* and *E* species of  $6.7 \pm 0.2$  K and of  $8.2 \pm 0.6$  K, respectively. They derived a total column density for CH<sub>3</sub>C<sub>3</sub>N of  $(1.74 \pm 0.1) \times 10^{12} \text{ cm}^{-2}$ . Hence, the CH<sub>3</sub>C<sub>3</sub>N/CH<sub>2</sub>DC<sub>3</sub>N abundance ratio is  $22 \pm 2$ .

The column density of CH<sub>3</sub>C<sub>4</sub>H has been derived by Cernicharo et al. (2021c) to be  $(1.30 \pm 0.04) \times 10^{13} \text{ cm}^{-2}$ . Assuming the same rotational temperature for CH<sub>2</sub>DC<sub>4</sub>H than for the main isotopologue (Cernicharo et al. 2021c), we derive a  $3\sigma$  upper limit to its column density of  $3.7 \times 10^{11} \text{ cm}^{-2}$ . Therefore, the CH<sub>3</sub>C<sub>4</sub>H over CH<sub>2</sub>DC<sub>4</sub>H abundance ratio is  $\geq 35$  ( $3\sigma$ ). For the deuterated species CH<sub>3</sub>C<sub>4</sub>D, for which laboratory spectroscopy is available (Heath et al. 1955), we derive a  $3\sigma$  upper limit to its column density of  $9 \times 10^{10} \text{ cm}^{-2}$ . Hence,  $N(\text{CH}_3\text{C}_4\text{H})/N(\text{CH}_3\text{C}_4\text{D}) \geq 144$ .

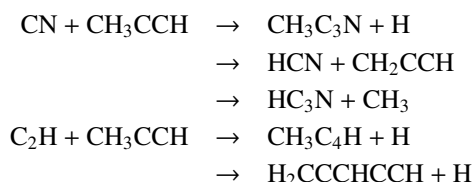
**Table 4.** Deuteration enhancement in TMC-1 for detected molecules compared to our gas phase chemical model.

Molecule	Observations	Model A	Model B
	TMC-1	no scrambling	full scrambling
CH <sub>3</sub> C <sub>3</sub> N/CH <sub>2</sub> DC <sub>3</sub> N	22 <sup>a</sup>	75.8	31.4
CH <sub>3</sub> CN/CH <sub>2</sub> DCN	11 <sup>b</sup>	15.0	15.0
H <sub>2</sub> CCN/HDCCN	20 <sup>b</sup>	23.6	23.6
HC <sub>3</sub> N/DC <sub>3</sub> N	62 <sup>c</sup>	54.9	54.5
HNCCC/DNCCC	43 <sup>c</sup>	34.6	34.5
HCCNC/DCCNC	30 <sup>c</sup>	27.2	27.1
HC <sub>5</sub> N/DC <sub>5</sub> N <sup>b</sup>	82 <sup>c</sup>	23.3	23.3
<i>c</i> -C <sub>3</sub> H <sub>2</sub> / <i>c</i> -C <sub>3</sub> HD	27 <sup>b</sup>	45.5	45.4
C <sub>4</sub> H/C <sub>4</sub> D	118 <sup>b</sup>	55.5	55.3
H <sub>2</sub> C <sub>4</sub> /HDC <sub>4</sub>	83 <sup>b</sup>	49.5	49.4
CH <sub>3</sub> CCH/CH <sub>3</sub> CCD	49 <sup>b</sup>	257	264
CH <sub>3</sub> CCH/CH <sub>2</sub> DCCH	10 <sup>b</sup>	76	76
CH <sub>3</sub> C <sub>4</sub> H/CH <sub>2</sub> DC <sub>4</sub> H	$\geq 35^d$	59	20
CH <sub>3</sub> C <sub>4</sub> H/CH <sub>3</sub> C <sub>4</sub> D	$\geq 144^d$	136	55

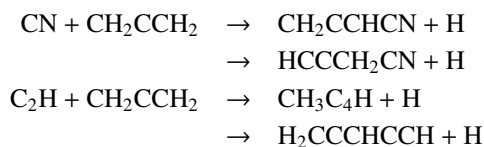
**Notes.** <sup>(a)</sup> This work. <sup>(b)</sup> Cabezas et al. (2021). <sup>(c)</sup> Cernicharo et al. (2020a). <sup>(d)</sup>  $3\sigma$  upper limit.

#### 4. Chemical Modelling

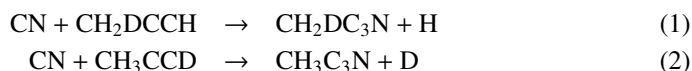
We further investigate the chemical processes leading to deuterium insertion in methylcyanoacetylene and methyldiacetylene, by extending our previous study on H<sub>2</sub>CCN and HDCCN (Cabezas et al. 2021). We only consider gas phase mechanisms which allow quantitative predictions based on some experimental measurements and theoretical studies. The chemistry of the different C<sub>4</sub>H<sub>3</sub>N and C<sub>5</sub>H<sub>4</sub> isomers has been discussed recently in Cernicharo et al. (2021c) and Marcelino et al. (2021) respectively, in relation with their detection in TMC-1. These both chemical families are tightly linked to the chemistry of methylacetylene, CH<sub>3</sub>CCH and its isomer allene, CH<sub>2</sub>CCH<sub>2</sub>.



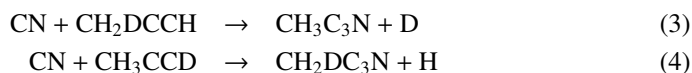
whereas



Considering the deuterated analogs of these reactions introduces diverse question marks, i.e., whether the CN reactions proceed without changing the methyl radical or lead to some scrambling of the hydrogen atoms in a quasi-stationary intermediate followed by different reaction channels. The first assumption would lead to the following reactions



whereas the second option would introduce an additional reaction channel:



The case of the reactions involving C<sub>2</sub>H (C<sub>2</sub>D) is even more uncertain as an additional H(D) atom is involved, which leads to a complementary reaction channel.



Similar questions arise in the deuteration mechanisms involving deuteron transfer initiated by reactions with abundant deuterated molecular ions such as H<sub>2</sub>D<sup>+</sup> and DCO<sup>+</sup>. As an example, the products of the H<sub>2</sub>D<sup>+</sup> + CH<sub>3</sub>C<sub>3</sub>N reaction could be CH<sub>3</sub>C<sub>3</sub>ND<sup>+</sup> + H<sub>2</sub> if the reaction proceeds directly or also CH<sub>2</sub>DC<sub>3</sub>NH<sup>+</sup> + H<sub>2</sub> if an intermediate complex is formed.<sup>3</sup> The following step to form deuterated methylcyanoacetylene entails dissociative recombination of the molecular ion, where an additional question arises on the branching ratios of the reaction CH<sub>2</sub>DC<sub>3</sub>NH<sup>+</sup> + e<sup>-</sup> → CH<sub>2</sub>DC<sub>3</sub>N + H or/and → CH<sub>3</sub>C<sub>3</sub>N + D. These few examples show the multiple issues that emerge when analyzing the potential chemical processes at work. We have considered two different approaches: In case A, we assume that the methyl radical and its deuterated form keep their structure (e.g. as in reactions 1, 2, 5, 6, 8) whereas case B involves a scrambling of the H and D atoms followed by the formation of the different products (e.g. as in reactions 3, 4, 7, 9, 10). These hypotheses are implemented in a chemical model including 320 species and more than 9000 gas phase reactions built from previous studies (Cabezas et al. 2021; Agúndez et al. 2021b). We display in Table 4 the corresponding steady state ratios obtained in a model adapted to TMC-1 conditions, n(H<sub>2</sub>) = 4 × 10<sup>4</sup> cm<sup>-3</sup>, T = 10 K, ζ = 1.3 × 10<sup>-17</sup> s<sup>-1</sup> as in Cabezas et al. (2021)<sup>4</sup>. We first notice the significant sensitivity of the deuterium ratio of CH<sub>3</sub>C<sub>3</sub>N and CH<sub>3</sub>C<sub>4</sub>H to the reactivity assumptions. A low deuterium fraction, close to the observed value of CH<sub>3</sub>C<sub>3</sub>N, is favored in the full scrambling approximation. The upper limits found for CH<sub>3</sub>C<sub>4</sub>H/CH<sub>2</sub>DC<sub>4</sub>H and CH<sub>3</sub>C<sub>4</sub>H/CH<sub>3</sub>C<sub>4</sub>D are on the other hand better reproduced when reactions 5, 6 and 8 are the only channels in the C<sub>2</sub>H (C<sub>2</sub>D) reactions. Whereas the other observed deuterium ratios are reasonably reproduced within a factor 2, a significant discrepancy is still obtained for methylacetylene, CH<sub>3</sub>CCH, as already noticed in Cabezas et al. (2021); Agúndez et al. (2021b). This feature arises because the reaction of CH<sub>3</sub>CCH with H<sub>3</sub><sup>+</sup> (and supposedly H<sub>2</sub>D<sup>+</sup>) leads to the break up of CH<sub>3</sub>CCH into *c*-C<sub>3</sub>H<sub>3</sub><sup>+</sup> and *l*-C<sub>3</sub>H<sub>3</sub><sup>+</sup> (*c*-C<sub>3</sub>H<sub>2</sub>D<sup>+</sup> and *l*-C<sub>3</sub>H<sub>2</sub>D<sup>+</sup>) rather than to C<sub>3</sub>H<sub>5</sub><sup>+</sup> or C<sub>3</sub>H<sub>4</sub>D<sup>+</sup> (CH<sub>3</sub>CCH<sub>2</sub><sup>+</sup>, CH<sub>2</sub>DCCH<sub>2</sub><sup>+</sup>, CH<sub>3</sub>CCHD<sup>+</sup>), as found in the experimental study of Milligan et al. (2002). We did not try to include additional deuterium exchange reactions, in the absence of any theoretical or experimental information.

We conclude this section by acknowledging the possible gas phase deuteration mechanisms of cyanomethylacetylene mediated by deuteron transfer reactions with species such as H<sub>2</sub>D<sup>+</sup>, DCO<sup>+</sup>, among other deuterated cations, in low temperature conditions but point out the substantial uncertainties involved in the different possible reactions, so that a detailed comparison between observations and chemical modeling appears elusive. A theoretical analysis of the intermolecular interaction potentials

involved in the approach of the different reactants would help to validate the various reaction mechanisms.

## 5. Conclusions

We have detected, and unambiguously identified, CH<sub>2</sub>DC<sub>3</sub>N in TMC-1, a new deuterated compound, thanks to highly sensitive space observations of 15 different transitions and associated theoretical considerations and quantum mechanical calculations. Spectroscopic constants are also provided for that compound and the <sup>13</sup>C and <sup>15</sup>N substitutes, which should help to study those species in the laboratory as well. The observed deuterium fractions are further compared to a gas phase model, which, despite significant uncertainties, accounts within a factor of two for the different values, except for CH<sub>3</sub>CCH. Further experimental or theoretical studies are welcome.

*Acknowledgements.* We thank ERC for funding through grant ERC-2013-Syg-610256-NANOCOSMOS. The Spanish authors thank Ministerio de Ciencia e Innovación for funding support through project AYA2016-75066-C2-1-P, PID2019-106235GB-I00 and PID2019-107115GB-C21 / AEI / 10.13039/501100011033. MA thanks Ministerio de Ciencia e Innovación for grant RyC-2014-16277. ER acknowledges the support of the Programme National 'Physique et Chimie du Milieu Interstellaire' (PCMI) of CNRS/INSU with INC/INP co-funded by CEA and CNES. Several kinetic data we used have been taken from the online databases KIDA (Wakelam et al. (2012), <http://kida.obs.u-bordeaux1.fr>) and UMIST2012 (McElroy et al. (2013), <http://udfa.ajmarkwick.net>).

## References

- Agúndez, M., Cabezas, C., Tercero B. et al. 2021a, A&A, 647, L10  
 Agúndez, M., Roueff, E., Cabezas, C., et al. 2021b, A&A, In press. DOI: <https://doi.org/10.1051/0004-6361/202140843>.  
 Broten, N. W., MacLeod, J. M., Avery, L. W., et al. 1984, ApJ, 276, L25  
 Brown, R. D., Brown, R. F. C., Eastwood, F. W., et al. 1979, J. Am. Chem. Soc. 101, 4705.  
 Cabezas, C., Endo, Y., Roueff, E., et al. 2021, A&A, 646, L1  
 Cazzoli, G., Cludi, L., Contento, M. & Pizzarini, C. 2008, J. Mol. Spectrosc., 251, 229  
 Cernicharo, J. 1985, Internal IRAM report (Granada: IRAM)  
 Cernicharo, J. 2012, in European Conference on Laboratory Astrophysics, eds. C. Stehlé, C. Joblin, & L. d'Hendecourt, EAS Publication Series, 58, 251  
 Cernicharo, J., Guélin, M., Agúndez, M., et al., 2018, A&A, 618, A4  
 Cernicharo, J., Marcelino, N., Agúndez, M., et al. 2020a, A&A, 642, L17  
 Cernicharo, J., Marcelino, N., Pardo, J. R., et al. 2020b, A&A, 641, L9  
 Cernicharo, J., Marcelino, N., Agúndez, M., et al. 2020c, A&A, 642, L8  
 Cernicharo, J., Cabezas, C., Agúndez, M., et al., 2021a, A&A, 648, L3  
 Cernicharo, J., Agúndez, M., Cabezas, C., et al. 2021b, A&A, 647, L2  
 Cernicharo, J., Cabezas, C., Agúndez, M., et al., 2021c, A&A, 647, L3  
 Cernicharo, J., Agúndez, M., Cabezas, C., et al. 2021d, A&A, 649, L15  
 Cernicharo, J., Cabezas, C., Endo, Y., et al. 2021e, A&A, 646, L3  
 Cernicharo, J., Cabezas, C., Bailleux, S., et al. 2021f, A&A, 646, L7  
 Cízek, J., in "Advances in Chemical Physics" (P. C. Hariharan, Ed.), Vol.14, 35, Wiley Interscience, New York, 1969  
 Dunning, T. H., 1989, J. Chem. Phys. 90, 1007  
 Fossé, D., Cernicharo, J., Gerin, M., Cox, P. 2001, ApJ, 552, 168  
 Kohguchi, H., Ohshima, Y., & Endo, Y. 1994, J. Chem. Phys. 101, 6463.  
 Heath, G.A., Thomas, L.F., Sherrard, E.I., & Sheridan, J. 1955, Faraday Soc. Disc., 19, 38  
 Hickson, K.B., Wakelam, V., Loison, J.C., 2016, Molec. Astrophys. 3, 1  
 Linsky, J. L. 2003, Space Sci. Rev., 106, 49  
 Marcelino, N., Cernicharo, J., Roueff, E., et al. 2005, ApJ, 620, 308  
 Marcelino, N., Tercero, B., N., Agúndez, M., & Cernicharo, J., et al. 2021, A&A, 646, L9  
 McElroy, D., Walsh, C., Markwick, A. J., et al. 2013, A&A, 550, A36  
 Milligan, D.B., Wilson, P.F., Freeman, C.G., et al. 2002, J. Phys. Chem. A, 106, 9745  
 Müller, H. S. P., Schlöder, F., Stutzki, J., & Winnewisser, G. 2005, J. Mol. Struct., 742, 215  
 Parise, B., Ceccarelli, C., Tielens, A. G. G. M., et al. 2006, A&A, 453, 949  
 Tang, J., Sumiyoshi, Y., & Endo, Y. 1999, Chem. Phys. Lett., 315, 69  
 Tercero, F., López-Pérez, J. A., Gallego, et al., 2021, A&A, 645, A37  
 Pardo, J. R., Cernicharo, J., Serabyn, E. 2001, IEEE Trans. Antennas and Propagation, 49, 12  
 Pickett, H. M., Poynter, R. L., Cohen, E. A., et al. 1998, J. Quant. Spectr. Rad. Transfer, 60, 883  
 Wakelam, V., Loison, J.-C., Herbst, E., et al. 2012, ApJS, 199, 21

<sup>3</sup> The channel CH<sub>3</sub>C<sub>3</sub>NH<sup>+</sup> + HD is present in both cases as well.

<sup>4</sup> The elemental values, i.e. O/H = 8 × 10<sup>-6</sup>, C/O = 0.75, N/O = 0.5 correspond to a carbon-rich environment.